Irreversible phase transitions driven by an oscillatory parameter in a far-from-equilibrium system

G. P. Saracco* and E. V. Albano†

Instituto de Investigaciones Fisicoquímicas Teóricas y Aplicadas (INIFTA), UNLP, CONICET, CIC (Buenes Aires), Casilla de Correo, 16 Sucursal 4, 1900 La Plata, Argentina

(Received 8 September 2000; published 26 February 2001)

The dynamic response of a forest-fire model to the harmonic variation of an external parameter is studied by means of numerical simulations. Second-order irreversible phase transitions driven by the harmonic input are reported. The location of such transitions depends on both the amplitude and period of the input signal. By means of epidemic studies the relevant critical exponents can be determined, which allow us to place the reported transitions in the universality class of directed percolation. This conclusion is also supported by a field theoretical calculation.

DOI: 10.1103/PhysRevE.63.036119 PACS number(s): 05.40.−a, 82.40.Bj, 64.60.Cn

I. INTRODUCTION

The study of the dynamic response of systems in thermodynamic equilibrium, close to reversible phase transitions to an external perturbation, is a subject of current interest [1–7]. Recent studies on the dynamic response of a classic Ising ferromagnet to an oscillatory magnetic field has led to the discovery of interesting phenomena such as dynamic hysteresis [1] and a fluctuation-induced symmetry breaking transition. Also, very recently, the dynamic response of an Ising system to a pulsed magnetic field was studied by means of Monte Carlo simulations and numerically solving a mean-field equation [7]. In a related context, the kinetic Ising model in an oscillating field exhibits a nonequilibrium dynamic phase transition [8]. Numerical Monte Carlo data of this system can be rationalized in terms of standard finite-size scaling arguments taken from the theory of second-order equilibrium phase transitions [8].

In contrast to their reversible counterpart, the study of the dynamic response of intrinsically irreversible systems close to irreversible phase transitions (IPT's) is still in its infancy. IPT's in an interacting particle system undergoing far from equilibrium conditions take place between an active (or reactive) regime and an inactive (or absorbing) state. Such transitions are irreversible because a system trapped in the absorbing state can never change its state. As in the case of equilibrium statistical physics, far from equilibrium processes are particularly interesting when the system undergoes irreversible phase transitions where particles behave collectively over long distances. Due to this interest the subject has been reviewed extensively; see, e.g., Refs. [9–11]. Among many systems exhibiting IPT's, directed percolation is one of the most studied models in nonequilibrium statistical physics (for pioneering reviews, see the works of Kinzel [12,13] and for a recent review see the e-print of Hinrichsen [14]). A summary of open problems in the field of directed percolation was recently published by Grassberger [15]. Other systems and models exhibiting IPT's are contact processes [9,11,17–20], branching annihilating walkers [21–25], forest-fire models [26–33], models of the dynamic evolution of living individuals [34], and several models of catalyzed reactions such as the Ziff-Gulari-Barshad (ZGB) model [35] and variations [36], the dimer-dimer model [37], the monomer-monomer model [35,38,39], etc.; for reviews on reaction systems, see, e.g., Refs. [40,41].

IPT's between an active regime and the absorbing state can be smooth (abrupt), and consequently they are classified as second (first) order. Very recently, we studied [42] the dynamic response of the ZGB model, close to its second-order IPT, to a pulsed perturbation. It is interesting to note that after driving a stationary configuration slightly into the absorbing state, the subsequent relaxation of the system can be well described by a stretched exponential behavior [42]. On the other hand, an oscillatory change in the input parameter (close to the first-order IPT in the ZGB model) considerably enhances the output of the product, and consequently the catalytic activity is improved [43]. Within this context, the aim of this work is to study the dynamic response of an irreversible system close to its second-order IPT, to an oscillatory change of the parameter. For this purpose, we have selected a forest-fire model with immune trees [26], which shows a very well characterized second-order IPT [27,28].

The manuscript is organized as follows: in Sec. II we describe the model and the simulation method. The theoretical background is briefly presented in Sec. III. Section IV is devoted to the presentation and discussion of our results. The conclusions are stated in Sec. V, and finally, field theoretical arguments supporting our findings are discussed in the Appendix.

II. MODEL AND DESCRIPTION OF THE SIMULATION TECHNIQUE

A. Forest fire model with immune trees

There is a great variety of forest-fire models (FFM's), [26–32]; for an extensive review see, e.g., Ref. [33]. Most FFM's are stochastic cellular automata which are defined on a d-dimensional hypercube lattice with L^d sites. Each site can be occupied by a tree, be occupied by a burning tree, or be empty. FFM's can be defined, giving a set of rules which

*Email address: gsaracco@inifta.unlp.edu.ar
†Email address: ealbano@inifta.unlp.edu.ar

are used during each Monte Carlo time step, to update the whole system in parallel. These rules can be summarized as follows:

(1) burning tree→empty site;
(2) tree→burning tree, with probability $(1-g)$ if at least one nearest neighbor (NN) is burning;
(3) empty site→tree with probability p;
(4) tree→burning tree, with probability f if no NN is burning.

Probability p is the growing probability, g is the immunity of each tree to catching fire, and f is the lightning probability which can be thought as the probability of spontaneous ignition of a tree. Of course the fire cannot propagate for $g=1$.

Qualitatively one expects that, if the immunity is nonzero, the fire fronts present for $g=0$ will become more and more fuzzy when increasing g; consequently the forest becomes denser. Taking $g=0$ and $f=0$ one has the model of Bak *et al.* [29], which is noncritical (in $d=2$) and exhibits a steady state, which is a succession of fire fronts with a fractal dimension $d=1$ [44]. Also, taking $g=0$ in the limit $f \ll 1$, $f/p \to 0$, one has the model proposed in Refs. [31–33], which shows self-organized critical (SOC) behavior. The paradigm of SOC behavior refers to the tendency of certain large dissipative systems to drive themselves into a critical state independent of the initial condition and without fine tuning of any parameter [45–47]. The occurrence of SOC behavior is the main reason for the popularity of sandpile and forest-fire models. Within this context, a very recent theoretical development deserves to be noticed. In fact, Broeker and Grassberger [48] reconsidered the FFM proposed by Bak *et al.* [45] not to be critical in two dimensions, but the model shows anomalous scaling in three and four dimensions. Also, the connection between SOC behavior and phase transitions in models with absorbing states was studied by Dickman *et al.* [49]. It was argued that SOC behavior can be understood as an aspect of multiple absorbing state systems under a slow drive [49]. A unified dynamic mean-field theory for stochastic SOC models was recently developed by Vespignani and Zapperi [50]. It was argued that, in a FFM with lightning, criticality arises in the limit of vanishing driving rates. From this perspective, SOC models appear to be nonequilibrium systems with steady states, and criticality may be reached by a fine tuning of the control parameters. However, in SOC systems such tuning can only be achieved by limit procedures [50]. Also, Sinha-Ray and Jensen [51] demonstrated that the stochastic FFM of Drossel *et al.* [31] can be turned into a deterministic threshold model with the same macroscopic statistical properties.

It is worth mentioning that FFM's exhibiting SOC behavior are not suitable for the present study on the influence of an oscillatory driven parameter, precisely because of the lack of tunable parameters. For this reason, in the present work we shall focus our attention on another kind of FFM, the so called forest-fire model with immune trees (FFMIT), which is defined by the above stated rules 1-3, and $f=0$ in rule 4. The FFMIT is simulated in a square lattice of linear size L, assuming periodic boundary conditions. Since the FFMIT is a cellular automaton, all sites are updated simultaneously during each Monte Carlo time step. Qualitatively speaking, if the growing probability is large ($p \to 1$, but $p<1$) and the immunity is low ($g \to 0$, but $g>0$) one expects the coexistence of fire, trees, and empty sites. However, keeping p constant and increasing g the fire will eventually cease and the system will become trapped in an absorbing state with the lattice completely filled by trees. So, the FFMIT exhibits second-order IPT's between an active state with fire propagation and an absorbing state where the fire becomes irreversibly extinguished [27,28]. Figure 1 shows the phase diagram of the FFMIT, i.e., a plot of the critical immunity (g_c) versus the critical grown probability (p_c), as obtained in previous works [27,28].

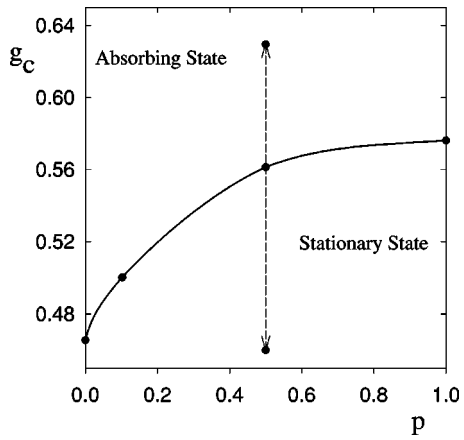

FIG. 1. Plot of the critical curve of the FFMIT, g_c vs p_c, valid in the thermodynamic limit $L=\infty$. The circle (●) shows the starting point of our simulations ($p_0=0.5, g_0=0.46$). The dotted line shows an example of variation of the parameter g according to Eq. (1).

B. A FFMIT with oscillatory variation of the parameters

An interesting approach to study the dynamic response of the FFMIT is to analyze its behavior upon temporal variations of the parameters. In principle, one can vary either p, g, or both of them simultaneously. However, for sake of simplicity, but without losing generality, we have worked taking $p=$ const while g is varied. For this purpose the procedure is as follows: first a stationary active state of the standard FFMIT is obtained for fixed values of the parameters. In this work we take $p_0=0.5$ and $g_0=0.46$, as shown in Fig. 1. Subsequently p is kept fixed ($p=p_0$), and g is varied harmonically according to

$$g=\left(g_0+\frac{A_g}{2}\right)+\frac{A_g}{2}\sin\left(\frac{2\pi}{T}t\right), \tag{1}$$

where A_g and T are the amplitude and the period of the oscillation, respectively. In order to drive the system into the absorbing state one has to take $A_g > g_c - g_0$, as shown in Fig. 1. Note that the critical point of the standard FFMIT is given by $p_0=p_c=0.5$ and $g_c=0.5614\pm0.0005$ [27,28].

C. Theoretical background

Due to the variation of the parameter [Eq. (1)], it is expected that for long enough periods and/or large amplitudes, the fire will eventually become extinguished, i.e., the system may be trapped in the absorbing state. So the periodic variation of g may cause IPT's between an active state with oscillations of fire and tree densities and the absorbing state with the sample filled with trees only. These transitions may occur at critical values of the amplitude A_{g_c} and the period T_c. In order to characterize and study such IPT's, epidemic simulations (ES's) have been performed.

The idea behind ES's is to start the runs from a configuration very close to the absorbing state, and subsequently, to follow the temporal evolution of the system under consideration. To do this, simulations are initiated with a sample filled with trees except for a small patch of 2×2 sites having burning trees and placed at the center of the lattice. Depending on the values of the parameters, such a small perturbation (fire) would either propagate or become extinguished. During the propagation, the following quantities are measured: (i) the average number of burning trees $N(t)$; (ii) the survival probability $P(t)$, i.e., the probability that the fire is still ignited at time t; and (iii) the average mean-square distance $R^2(t)$ over which the fire has spread. Note that $N(t)$ is averaged over all samples, including those in which the fire has already been extinguished, while $R^2(t)$ is averaged over samples having burning trees only. Averages are taken over 5000 different samples, and runs are performed up to 100 input periods. Simulations are performed in two dimensions, and the lattice size is selected large enough, usually $L=350$ or 500 lattice units (LU's), in order to avoid fire reaching boundaries. Using this procedure data are free of finite-size effects. The usual ansatz for epidemic simulation close to second order IPT's is to assume that $N(t)$, $P(t)$, and $R^2(t)$ obey a power-law dependency with exponents η, δ, and z, respectively. In the present ES the input parameter varies harmonically [see Eq. (1)], so we expect to obtain an oscillatory output modulated by a power law, that is

$$N(t)=N_o+t^{\eta}\left[N_1+N_2\cos\left(\frac{2\pi}{T}t+B\right)\right], \qquad (2)$$

where B is a constant phase shift, N_o is the initial number of burning trees, and N_1 and N_2 are constants. Similar laws are expected to hold for $P(t)$ and $R(t)$, respectively.

III. RESULTS AND DISCUSSION

As already stated, standard simulations were performed achieving a stationary reactive state for the standard FFMIT taking $p_0=0.5$ and $g_0=0.46$, as shown in Fig. 1. Subsequently, the harmonic variation of the immunity is switched on, according to Eq. (1). Figure 2 displays two typical examples of the observed behavior. Starting from the same initial configuration, the system is driven by two different oscillatory signals, both with the same period $T=55$ MCS's [in all figures, the time is measured in Monte Carlo steps (MCS's)], but with different amplitudes. Taking $A_g=0.1650$ [Fig. 2(a)], one sees that the system is effectively driven into the absorbing state ($g_0+A_g=0.625>g_c=0.5614$). However, since A_g is not too large the system reaches a time-dependent oscillatory regime with the coexistence of fire, trees, and empty sites. In contrast, increasing the amplitude up to $A_g=0.1695$ [Fig. 2(b)], after a few oscillations the system finally becomes trapped in the absorbing state with fire extinction. Note that at least three cycles in Fig. 2(b) exhibit a very small amount of burning trees when the system is driven within the absorbing state. In these cases the fire recovers during the remaining half cycle. Of course, due to the vanishing small amount of fire, a fluctuation would eventually cause fire extinction, as shown in Fig. 2(b).

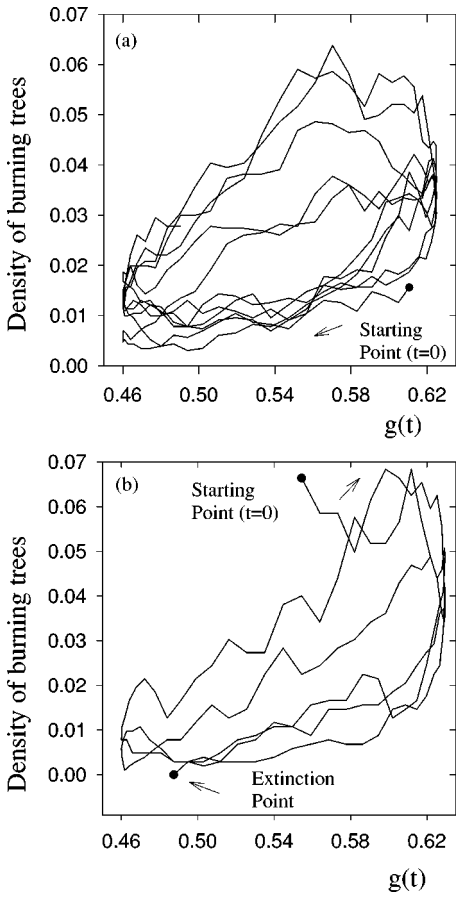

FIG. 2. Plots of the density of burning trees versus the input signal $g(t)$ taken for $p_0=0.5$,$T=55$ Monte Carlo steps (MCS's), and using lattices of $L=400$ lattice units (LU's). In (a) the amplitude is $A_g=0.1650$, and the system oscillates indefinitely. In (b) one has $A_g=0.1695$, and the system evolves toward the irreversible extinction of the fire.

In order to obtain the precise location of the critical point; namely, the critical amplitude A_{g_c} and the critical period T_c, ES's have been performed. In fact, determinations of critical points using standard measurements of the dependences of $N(t)$ versus $g(t)$, e.g., as shown in Fig. 2, are heavily affected by fluctuations of the stochastic system and undesired finite-size effects. Figure 3(a) shows a log-log plot of $N(t)$ versus t obtained performing ES's where the oscillatory output can clearly be observed. In order to perform a preliminary fit, we have first determined the values of $N(t)$ on

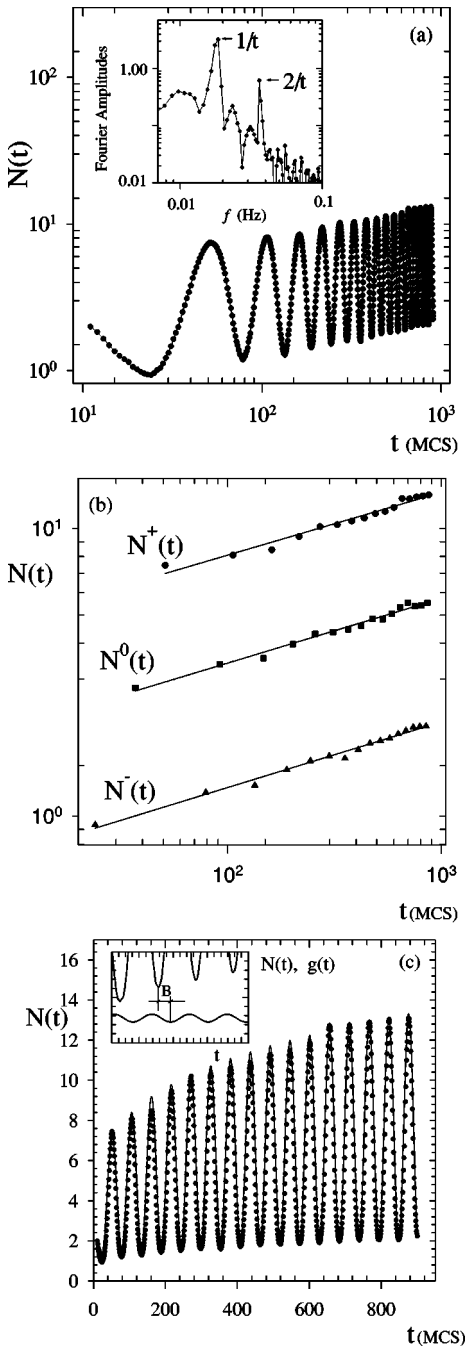

FIG. 3. (a) Log-log plot of the number of burning trees $N(t)$ vs t, exhibiting the features exposed in the theoretical background. Results obtained at criticality, viz. $A_{g_c}=0.1695$, where $T_c=55$ MCS's. The envelope shows a linear positive slope, characteristic of second-order IPT. The inset shows the results of a Fourier analysis through an amplitude spectrum of the time series of $N(t)$ at criticality. The location of the first harmonics are shown by arrows. More details in the text. (b) Log-log plot of maximum, minimum, and approximately medium points of $N(t)$ are taken from Fig. 3(a) vs t. The linear dependence allows us to determine the exponents reported in the text. (c) Plot of the number of burning trees vs t fitted by the ansatz proposed in Eq. (2). The inset shows the plot of $N(t)$ and $g(t)$ vs t, which allows us to determine the constant phase shift B.

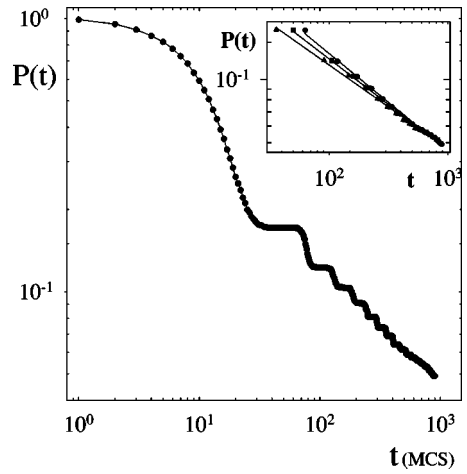

FIG. 4. Log-log plot of the survival probability $P(t)$ versus t at the critical point $A_{gc}=0.1695$, where $T_c=55$ MCS's. The oscillatory shape is clearly observed. The inset shows the linear fit of peaks, valleys, and medium points. For more details, see the text.

peaks, valleys and centers, given by N^+, N^-, and N^0, respectively. Figure 3(b) shows that log-log plots of N^+, N^-, and N^0 versus t can be very well fitted by straight lines with slopes $\eta^+=0.22\pm0.02$, $\eta^-=0.22\pm0.02$, and $\eta^0=0.22\pm0.02$, respectively. Plots drawn taking a smaller (larger) amplitude show an upward (downward) curvature suggesting that they are off critically. Precisely, the straight lines exhibited in the log-log of Fig. 3(b) are the signature of a power-law behavior which characterizes a second-order phase transition exhibiting scale invariance. The inset in Fig. 3(c) shows that it also is possible to determine the assumed constant phase shift in equation (2), by comparing plots of $N(t)$ and $g(t)$ versus t. For example in Fig. 3(c) $B=1.37\pm0.34$ has been obtained. It should be noticed that B remains constant, within error bars, for the whole time series of $N(t)$ versus t, in agreement with the lack of evidences of anharmonic terms found using the Fourier analysis [Fig. 3(a)]. Therefore it is now possible to fit the whole curve of $N(t)$ versus t using the already determined values of η and B, keeping $N_o=1.0$ fixed (because in principle, only one tree is needed to start the epidemic), but taking N_1 and N_2 as adjustable parameters, as shown in Fig. 3(c), with $N_1=1.3\pm0.1$ and $N_2=1.09\pm0.06$.

Figure 4 shows that a log-log plot of $P(t)$ versus t also exhibits oscillatory behavior. Here, the survival probability is due to the increment in the immunity which makes the fire propagation harder and may cause the eventual extinction of some epidemics. Defining the maximum, minimum, and medium values of $P(t)$ in each cycle as P^+, P^-, and P^0, respectively, one can obtain the exponent δ, as shown in the inset of Fig. 4. Our results, at criticality, are $\delta^+=0.46\pm0.02$, $\delta^-=0.40\pm0.04$ and $\delta^0=0.43\pm0.03$, respectively. This finding suggests that $\delta^+=\delta^0=\delta^-$ considering both error bars and finite time corrections.

Figure 5 shows a log-log plot of R^2 versus t obtained for $T_c=55$ MCS's and $A_{g_c}=0.1695$. It is found that R^2 is less sensitive to the oscillatory input than $N(t)$ and $P(t)$. This behavior is due to the fact that $R^2(t)$ only accounts for sur-

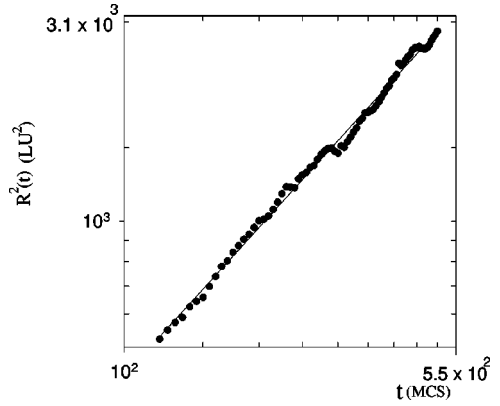

FIG. 5. Log-log plot $R^2(t)$ (measured in lattice units, Lu^2) versus t. Here the oscillations have been heavily damped, and the points are roughly fitted by a straight line with slope $z=1.18\pm0.06$.

viving epidemics at time t. The plot can roughly be fitted by a straight line which yields a slope $z\cong1.18\pm0.06$.

It should be noticed that the evaluated exponents are universal properties of the model that define its universality class. These relevant figures have to be clearly distinguished from non-universal properties such as, e.g., the oscillatory behavior of $N(t)$ and $P(t)$ and the constant phase shift B. Having these concepts in mind, we conclude that all the dynamic exponents that characterize the IPT's driven by the oscillatory parameter are in agreement with those of the universality class of directed percolation (DP) in $2+1$ dimensions, namely, $\eta=0.22\,295(10)$, $\delta=0.4505(10)$, and $z=1.1325(10)$ [16]. Also, the hyperscaling relation $dz=4\delta+2\eta$, where $d=2$ is the lattice dimension, is well satisfied by these exponents. So we conclude that the type of transition discussed so far can be placed in the universality class of DP (a formal treatment performed by Muñoz [52] can be found in the Appendix). This result extends the validity of Janssen's conjecture [53], that a continuous transition into an absorbing state characterized by a scalar order parameter must belong to the universality class of DP, to irreversible transitions driven by oscillatory parameters. Recently such a conjecture was extended to systems with an infinite number of absorbing states [54,55] and to second-order transitions in continuous media [56].

Performing ES with different values of A_g and T, the phase diagram of the FFMIT under oscillatory driving has been evaluated, as shown in Fig. 6. The critical curve A_{g_c} versus T_c shows the location of second-order IPT's between the active regimes (trees + burning trees + empty sites) and the absorbing state (only trees). All these transitions are of second order, and belong to the universality class of DP. The inset of Fig. 6 shows a log-log plot of T_c versus $\Delta A=A_{g_c}-(g_c-g_0)$. Note that ΔA is the ''excess critical amplitude,'' namely, a renormalized amplitude which accounts for the value of the oscillatory parameter which exceeds the stationary critical threshold, allowing the system to make an excursion to an absorbing state. The data are then consistent with a hyperboliclike behavior of the form $T_c\propto\Delta A^{\alpha}$, with exponent $\alpha\cong4.55$. The deviation from this behavior, observed for

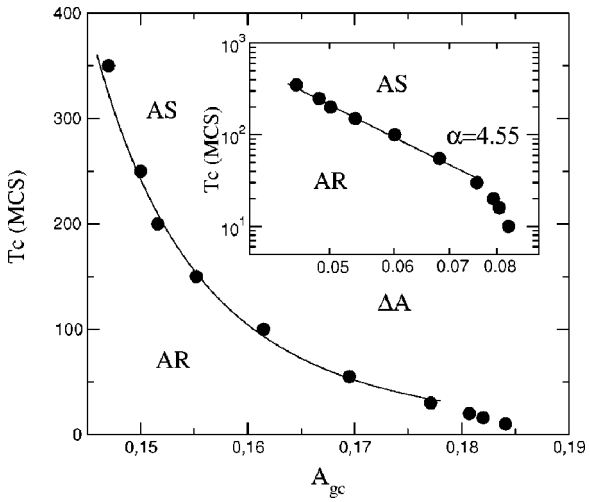

FIG. 6. Phase diagram of the FFMIT under periodic oscillations. The plane $\{A_g,T\}$ is divided by the critical curve, which shows the precise location of second-order IPT's as determined by ES's. Each point on the curve belongs to the directed percolation universality class. The absorbing state (AS) and the active regime (AR) are shown. The hyperboliclike shape of the curve is displayed as the log-log plot in the inset, giving an exponent $\alpha\cong4.55$. More details are given in the text.

short periods, is likely due to the fact that the input signal can no longer be considered as harmonic.

The dynamic response of the FFMIT to a rectangular perturbation, instead of the sinusoidal input given by Eq. (1), has also been studied. Figure 7 shows a log-log plot of $N(t)$ versus t obtained at criticality. In contrast to Fig. 3(a) where $N(t)$ exhibits smooth oscillations, the response to the rectangular input is characterized by sharp edges. The inset shows

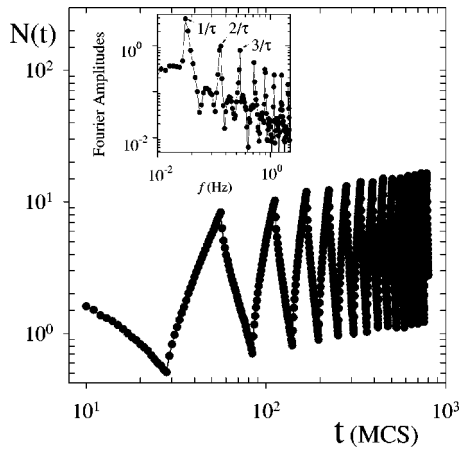

FIG. 7. Log-log plot of $N(t)$ vs t as obtained by using for rectangular input at the critical point $A_{g_c}=0.1534$, where $T_c=56$ MCS's. Oscillations are observed as in the case of sinusoidal signal, but in the present case they have a saw tooth shape. The envelope is linear, showing the expected power-law behavior. The Fourier analysis of the output has also been performed, and the result is shown in the inset. Note, in contrast to the sinusoidal case, the appearance of additional harmonic terms, needed to build the abrupt edges.

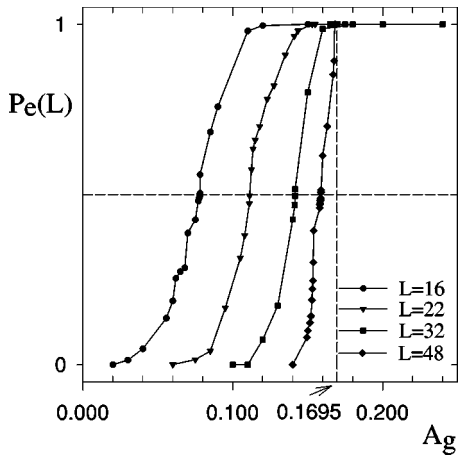

FIG. 8. Plot of $P_e(L)$ vs A_g obtained for samples of different sizes L. The smooth ''s'' shapes steadily approach to the abrupt jump $P_e(L=\infty)$ at $A_g(L=\infty)=0.1695$ (vertical line). The horizontal line indicates the location of $P_e(L)=0.5$, which is defined as the L-dependent critical probability. For more details see the text.

the corresponding Fourier analysis, which reveals that, in this case, it is necessary for more harmonic terms to build up the output due to the abrupt edges of the input square signal. Fitting the maximum, medium, and minimum values of $N(t)$ versus t, we have obtained $\eta^+=0.22\pm0.04$, $\eta^-=0.22\pm0.04$, and $\eta^0=0.22\pm0.04$, respectively. This and results of other ES's (not shown here for the sake of space) allow us to conclude that second-order IPT's driven by rectangular perturbation also belong to the universality class of DP. As expected, the location of the critical curve becomes shifted as compared with the sinusoidal input, shown in Fig. 6. In fact, keeping the period constant one sees that critical amplitudes of the rectangular input are slightly smaller than those corresponding to the sinusoidal input.

Another approach to the study of dynamic response is to perform simulations within the reactive regime (see Fig. 6) and close to the critical edge. In this case, the fact that fluctuations of the stochastic system may irreversibly drive it into the absorbing state can be used. Thus $P_e(L)$ is defined as the probability of fire extinction in a lattice of side L. Figure 8 shows plots of $P_e(L)$ versus the amplitude of the input signal, corresponding to samples of different sides. In this case the period of the oscillation is kept fixed at $T=55$ MCS's. Figure 8 also shows the location of the critical amplitude in the thermodynamic limit $A_{g_c}(L=\infty)=0.1695$, as determined by means of ES's. In contrast to the stepwise and abrupt change of $P_e(\infty)$ from 0 to 1 which takes place right at $A_{g_c}(\infty)$, using finite samples one observes smooth variations of $P_e(L)$ which steadily approach to the stepped shape when L is increased. The L-dependent *critical* amplitude of a finite sample $[A_{g_c}(L)]$ is defined for $P_e(L)=0.5$ (also see Fig. 8). According to the finite-size scaling theory [57],

$$A_{g_c}(L)=A_{g_c}(\infty)+ML^{-1/\nu_\perp} \tag{3}$$

where M is a constant and $\nu_\perp$ is the correlation length exponent in the spatial direction.

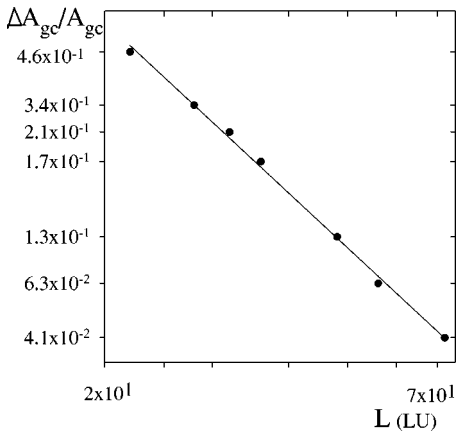

FIG. 9. Log-log plot of ΔA vs L obtained assuming $A_g=0.1794$. This value renders the correct correlation length exponent $\nu_\perp=0.729$ given by the slope of the straight line. For more details, see the text.

Figure 9 shows a log-log plot of $\Delta A=A_{g_c}(\infty)-A_{g_c}(L)$ versus L. In order to obtain a critical exponent compatible with the DP universality class, namely, $\nu_\perp=0.729$ [16] one has to assume $A_{gc}=0.1794$, which represents a very small shift of 0.009 to the previous estimation of $A_{gc}=0.1695$, obtained by means of ES. So, conclude that our finite-size study is consistent with the ES and the transition belongs to the universality class of directed percolation [16].

IV. CONCLUSIONS

The dynamic response of a forest fire model with immune trees to an oscillatory variation of the input parameter has been studied. Second-order irreversible phase transitions driven by an oscillatory parameter are found. The critical edge between an active state with fire fronts and an absorbing state where the fire becomes extinguished depends on the amplitude and the period of the harmonic input. The transition points were located accurately by means of epidemic studies. All irreversible transitions were found to belong to the universality class of directed percolation. Our studies, performed in a forest-fire model, can be straightforwardly extended to other processes exhibiting irreversible phase transitions, such as, e.g., catalyzed reaction systems, contact processes, models of living societies, branching annihilating walkers, etc. We also expect that our numerical results will further stimulate the study of the dynamic response of systems close to irreversible transitions, an interesting topic which remains almost unexplored.

ACKNOWLEDGMENTS

This work is financially supported by CONICET, UNLP, ANPCyT, Fundación Antorchas (Argentina), and the Volkswagen Foundation (Germany). We are very grateful to M. A. Muñoz for his significant theoretical contribution.

APPENDIX: FIELD THEORETICAL ARGUMENTS ON THE OSCILLATING IMMUNITY FOREST FIRE MODEL

In the presence of a constant immunity rate the critical aspects of the forest-fire model and/or other epidemic models

with partial immunization can be described by reggeon field theory [58,59]. Therefore, all these models share their critical universal properties with directed percolation [11]. The minimal Langevin equation capturing the physics at criticality is [11,58].

$$\frac{\partial \phi(\mathbf{x},t)}{\partial t} = \lambda \nabla^2 \phi(\mathbf{x},t) + r\,\phi(\mathbf{x},t) - b\,\phi^2(\mathbf{x},t) + \sqrt{\phi}\,\eta(\mathbf{x},t) \tag{A1}$$

where λ, r, and b are constants, $\phi(\mathbf{x},t)$ is a density field, and η is a Gaussian white noise whose only nonvanishing cumulants are $\langle \eta(\mathbf{x},t)\,\eta(\mathbf{x}',t')\rangle = D\,\delta(\mathbf{x}-\mathbf{x}')\,\delta(t-t')$.

The most relevant modification induced by switching on a periodic immunity rate at this level is that r has to be replaced by a time dependent function: $r \to r_0 + A\cos(wt)$. Following the renormalization group spirit we can integrate out short times and space scales. In this way, integrating Eq. (A1) in time over a signal period $T = 2\pi/w$, dividing by T, and defining a new order parameter

$$Q(x,\tau) = \frac{1}{T}\int_0^T dt\ \phi(\mathbf{x},\mathbf{t}) \tag{A2}$$

(with $\tau = t/T$), one obtains

$$\frac{\partial \phi(\mathbf{x},t)}{\partial t} = \lambda \nabla^2 Q(\mathbf{x},\tau) + r_0 Q(\mathbf{x},\tau) - b\int_0^T \phi^2(\mathbf{x},t)\,dt + \int_0^T \sqrt{\phi}\,\eta(\mathbf{x},t). \tag{A3}$$

As on these short time scales, there are no anomalous, critical, fluctuations, we can safely substitute variables with their mean values, averaged over a time period (at least as long as one deals with large scale, asymptotic properties). Therefore, Eq. (A3) can be rewritten as

$$\begin{aligned}\frac{\partial Q(\mathbf{x},t)}{\partial \tau} &= \lambda \nabla^2 Q(\mathbf{x},\tau) + \mathbf{r}_0 \mathbf{Q}(\mathbf{x},\tau) - \mathbf{b}\mathbf{Q}(\mathbf{x},\tau)\int_0^{\mathbf{T}} \phi(\mathbf{x},\mathbf{t})\,\mathbf{dt} \\ &\quad + \sqrt{Q}\int_0^T \eta(\mathbf{x},\mathbf{t})\,\mathbf{dt} \\ &= \lambda \nabla^2 Q(\mathbf{x},\tau) + \mathbf{r}_0 \mathbf{Q}(\mathbf{x},\tau) - \overline{\mathbf{b}}\mathbf{Q}^2(\mathbf{x},\tau) + \sqrt{Q}\,\xi(\mathbf{x},\mathbf{t}),\end{aligned} \tag{A4}$$

where we have defined a Gaussian noise $\xi(\mathbf{x},\tau)$ as the averaged value of $\eta(\mathbf{x},t)$ over a period, and $\overline{b} = bT$. We have a reggeon field theory equation, identical to Eq. (A1), where $\phi(\mathbf{x},t)$ is replaced by $Q(\mathbf{x},\tau)$. Consequently, *all the critical exponents associated with* $Q(\mathbf{x},\tau)$ *are expected to take directed percolation values*.

Observe that for any value of t for which $\cos(wt)$ is positive, the system is locally in time in the active phase; therefore, a growth on the averaged value of ϕ is expected at that time. The system returns (locally in time) to the absorbing phase whenever $\cos(wt) \leqslant 0$; i.e., at these values, magnitudes like, e.g., $N(t)$ start to decrease. Zeros of the signal correspond to extrema of the output. This fact provides a simple explanation for the presence of dephasing between input and output signals, as shown in Fig. 3(c).

[1] M. Rao, H.R. Krishnamurty, and R. Pandit, Phys. Rev. B **42**, 856 (1990).

[2] W.S. Lo and R.A. Pelcovits, Phys. Rev. A **42**, 7471 (1990).

[3] M.F. Zimmer, Phys. Rev. E **47**, 3950 (1993).

[4] M. Acharyya and B.K. Chakrabarti, Phys. Rev. B **52**, 6550 (1995).

[5] A. Fierro, A. de Candia, and A. Coniglio, Phys. Rev. E **56**, 4990 (1997).

[6] M. Acharyya, J.K. Bhattacharje, and B.K. Chakrabarti, Phys. Rev. E **55**, 2392 (1997).

[7] M. Acharyya, Phys. Rev. E **56**, 2407 (1997).

[8] S.W. Sides, P.A. Rihvold, and M.A. Novotny, Phys. Rev. E **59**, 2710 (1999).

[9] T.M. Ligget, *Intereacting Particle Systems* (Springer, Berlin, 1988).

[10] N. Konno, *Phase Transitions of Interacting Particle Systems* (World Scientific, Singapore, 1994).

[11] J. Marro and R. Dickman, *Nonequilibrium Phase Transitions in Lattice Models* (Cambridge University Press, Cambridge, 1998); G. Grinstein and M.A. Muñoz, in *Fourth Granada Lectures on Computational Physics*, edited by P.L. Garrido and J. Marro, Lecture Notes in Physics Vol 493 (Springer, Berlin, 1997), p. 223.

[12] W. Kinzel, in *Percolation Structures and Processes*, edited by G. Deutscher, R. Zallen, and J. Adler, Annals of the Israel Physical Society Vol. 5 (Hilger, Bristol, 1983).

[13] W. Kinzel, Z. Phys. B: Condens. Matter **58**, 229 (1985).

[14] H. Hinrichsen, E-print, cond-mat/0001070.

[15] P. Grassberger, in *Nonlinearities in Complex Systems, Proceedings of the 1995 Shimla Conference on Complex Systems* (Narosa, New Dehli, 1997).

[16] M.A. Muñoz, R. Dickman, A. Vespigiani, and S. Zapperi, Phys. Rev. E **59**, 6175 (1999).

[17] M. Hoyuelos, H.O. Martin, and E.V. Albano,, J. Phys. A **30**, 431 (1997).

[18] R. Dickman and I. Jensen, Phys. Rev. Lett. **67**, 2391 (1991).

[19] I. Jensen, Phys. Rev. A **45**, R563 (1992); Phys. Rev. Lett. **70**, 1465 (1993).

[20] I. Jensen and R. Dickman, J. Phys. A **26**, L151 (1993); Physica A **203**, 175 (1994).

[21] H. Takayasu and A.Yu Tretyakov, Phys. Rev. Lett. **68**, 3060 (1992).

[22] I. Jensen, Phys. Rev. E **47**, 1 (1993); J. Phys. A **26**, 3921 (1993); Phys. Rev. E **50**, 3623 (1994).

[23] D. Bem-Avraham, F. Leyvraz, and S. Redner, Phys. Rev. E **50**, 1843 (1994).

[24] J. Cardy and U. Tauber, Phys. Rev. Lett. **77**, 4870 (1996); J. Stat. Phys. **90**, 1 (1998).

[25] E.V. Albano, M. Hoyuelos, and H.O. Martin, Physica A **239**, 531 (1997).
[26] B. Drossel and F. Schwabl, Physica A **199**, 183 (1993).
[27] E.V. Albano, J. Phys. A **27**, 881 (1994).
[28] E.V. Albano, Physica A **216**, 213 (1995).
[29] P. Bak, K. Chen, and C. Tang, Phys. Lett. A **147A**, 297 (1990).
[30] K. Christensen, H. Flyvbjerg, and Z. Olami, Phys. Rev. Lett. **71**, 2737 (1993).
[31] B. Drossel, S. Clar, and F. Schwabl, Phys. Rev. Lett. **71**, 3739 (1993).
[32] W. von Niessen and A. Blumen, Can. J. Forest Res. **18**, 805 (1988); J. Phys. A **19**, L289 (1986).
[33] S. Clar, B. Drossel, and F. Schwabl, J. Phys.: Condens. Matter **8**, 6803 (1996).
[34] R.A. Monetti and E.V. Albano, Physica A **234**, 785 (1997).
[35] R.M. Ziff, E. Gulari, and Y. Barshad, Phys. Rev. Lett. **56**, 2553 (1986).
[36] K. Yaldran and M.A. Khan, J. Catal. **131**, 369 (1991).
[37] E.V. Albano, J. Phys. A **25**, 2557 (1992); A. Maltz and E.V. Albano, Surf. Sci. **227**, 414 (1992).
[38] E.V. Albano, Phys. Rev. Lett. **69**, 656 (1992).
[39] P. Meakin and D.J. Scalapino, J. Chem. Phys. **87**, 731 (1987).
[40] E.V. Albano, Heterog. Chem. Rev. **3**, 389 (1986).
[41] V.P.Z. Zhdanov and B. Kasemo, Surf. Sci. Rep. **20**, 111 (1994).
[42] E.V. Albano, Eur. Phys. J. B **9**, 685 (1999).
[43] A. Lopez and E.V. Albano, J. Chem. Phys. **112**, 8, 3890 (2000).
[44] P. Grassberger and H. Kantz, J. Stat. Phys. **63**, 685 (1991).
[45] P. Bak, C. Tang, and K. Weisenfeld, Phys. Rev. Lett. **59**, 381 (1987); Phys. Rev. A **38**, 364 (1988).
[46] P. Bak, in *How Nature Works* (Springer, New York, 1996).
[47] H.J. Jensen, in *Self-Organized Criticality: Emergent Complex Behavior in Physical and Biological Systems* (Cambridge University Press, Cambridge, England, 1998).
[48] H.-S. Broeker and P. Grassberger, Phys. Rev. E **56**, R4918 (1997).
[49] R. Dickman, A. Vespignani, and S. Zapperi, Phys. Rev. E **57**, 5095 (1998).
[50] A. Vespignani and S. Zapperi, Phys. Rev. E **57**, 6345 (1998).
[51] P. Sinha-Ray and H.J. Jensen, Phys. Rev. E **62**, 3215 (2000).
[52] M.A. Muñoz (private communication).
[53] H.K. Janssen, Z. Phys. B: Condens. Matter **42**, 151 (1981).
[54] I. Jensen and R. Dickman, Phys. Rev. E **48**, 1710 (1993).
[55] E.V. Albano, Physica A **214**, 424 (1995).
[56] D. Linares, E.V. Albano, and R. Monetti, J. Phys. A **32**, 8023 (1999). published).
[57] D. Stauffer and A. Aharony, *Introduction to Percolation Theory*, 2nd ed. (Taylor & Francis, London, 1992).
[58] J.L. Cardy and R.L. Sugar, J. Phys. A **13**, L423 (1980); H.K. Janssen, Z. Phys. B: Condens. Matter **42**, 151 (1981); P. Grassberger, *ibid.* **47**, 365 (1982).
[59] The case of total or perfect inmunization is different; in that case the critical behavior is controlled by dynamical standard (isotropic) percolation. See H.K. Janssen, Z. Phys. B: Condens. Matter **58**, 311 (1985). Also see J.L. Cardy, J. Phys. A **16**, L709 (1983).